Materials Transactions, Vol. 49, No. 6 (2008) pp. 1380 to 1384

Effect of CH/C_2 Species Density on Surface Morphology of Diamond Film Grown by Microwave Plasma Jet Chemical Vapor Deposition

Chun-Hsi Su and Ching-Yu Chang*

Graduate Institute of Mechanical and Electrical Engineering, National Taipei University of Technology, Taipei 10643, Taiwan, R.O. China

The present research employs *in-situ* plasma Optical Emission Spectroscopy (OES) to explore the effect of microwave plasma jet chemical vapor deposition (MPJCVD) on activating $CH_4 + H_2$ plasma environment and synthesizing diamond film. Surface morphology and main orientation of lattice plane of the diamond synthesized under different processing parameters are also examined. Since species such as CH, H_2, hydrogen Balmer alpha (H_α), carbon dimer (C_2) and hydrogen Balmer beta H_β in the plasma radical are easily influenced by gas concentration, substrate temperature and processing parameters, *in-situ* OES is employed to diagnose *in-situ* OES diagnosing is employed to composition of plasma species in the synthesis of diamond film. Our findings reveal that species such as CH, C_2 and H_β in microwave plasma jet have significant influence on grain size, surface morphology and H/C carbon concentration. The Raman spectrum measurement can prove the relationship between CH/C_2 species density and diamond surface morphology. [doi:10.2320/matertrans.MRA2007324]

(Received December 12, 2007; Accepted February 25, 2008; Published April 16, 2008)

Keywords: *diamond, nanocrystalline diamond, mechanism, optical emission spectroscopy (OES), Raman spectrum*

1. Introduction

According to the energy-based reaction involved, the methods of synthesizing diamond and nanocrystalline diamond film through chemical vapor deposition (CVD) can be classified into three types. They are hot filament CVD, microwave plasma CVD and direct current CVD,[1–3] in which microwave energy is utilized to generate, control and concentrate plasma. Microwave plasma is characteristic of good electric coupling, stability and homogeneity. Moreover, the external electric pole is not involved, resulting in minimal damage to coating caused by the ion and electron generated in microwave plasma.[4] Nevertheless, microwave plasma CVD-based diamond film still raises problems such as low deposition rate and unstable plasma. With regard to the strength of plasma, Mitsuda *et al.* succeeded in developing highly densed and stable plasma diamond film using MPJCVD.[5]

Chemical research on plasma leads to the evidence that CH_3 radical is the precursor for growing multiple crystalline diamond film[6] while C_2 dimer plays an important role in synthesizing nanocrystalline diamond film.[7] Moreover, H proton is capable of etching, activating and stabilizing graphite.[3] A better understanding of the composition of plasma species, comprising both active and neutral reactive species and intermediates, in the preparation of diamond film will shed light on the optimization, nucleation and growth mechanism of diamond film. *In-situ* plasma OES is a non-intrusive high-sensitivity detector that can ensure easy identification of chemical species. In addition, it can provide high-resolution analysis of time and frequency domains, and is therefore most suitable for application to *in-situ* plasma diagnosis.

Previous studies have reported the influence of C_2 species on diamond and nanocrystalline diamond film under pressure ranging from 1.34 to 13.4 kPa.[8] When growing diamond with gases including $C_{60}/Ar/H_2$, CH_4/Ar, CH_4/N_2 and CH_4/H_2 as well as processing nanocrystalline diamond film, Zhou *et al.* discovered that C_2 will contribute to the formation of diamond phase and the increase nucleation.[9–11] In addition, Hiramatsu *et al.*[12] succeeded in utilizing plasma absorption spectrophotometer to detect the C_2 radical density at the lowest excited state ($a^3\Pi_u$), and to establish the relationship between C_2 specie density and nanocrystalline diamond film growth.

In the present study, OES is employed to conduct *in-situ* measurement of diamond and nanocrystalline diamond film grown by MPJCVD. The relationship between C_2 specie density and diamond surface morphology is discussed, so are the relationships between the orientation of diamond lattice plane (111)/(220) and all plasma species.

2. Experimental Details

Various types of diamond, nanocrystalline diamond and lamella graphite are synthesized using different CH_4/H_2 plasmas from 0.2% to 99%. The relationships between different diamond surface morphologies and lattice orientation have been discussed.[13] The MPJCVD is employed to grow diamond film on Si(100) substrate and the system transmits 700 W microwave to the antennal tip via a conical slow-wave structural antennal. When 200 sccm of CH_4/H_2 gas from 0.2% to 99% is introduced, the plasma beam will be jetted at the pressure of 4.69 kPa for 60 min to synthesize diamond film. The characterization of diamond film is analyzed using Raman spectroscopy (RENISHAW in Via, Ar^+ laser emitting 10 mW at 514 nm wavelength was used for the analysis), scanning electron microscopy (SEM) (LEO 1530) and X-ray diffraction (Rigaku D/max-B Cu K_α radiation). The Raman spectrum consists of the microcrystalline diamond (MCD) peak (1332 cm^{-1}, D_f-peak), the carbon peak (1350 and 1580 cm^{-1}, D and G peak), and the nanocrystalline diamond (NCD) peak (1150 and 1490 cm^{-1}, D^* and G^* peak). The X-ray diffraction pattern shows prominent peaks at angles of 43.34, 74.68, 90.36 and 118.37° which correspond to the normal structure factor of diamond

*Ph. D candidate, National Taipei University of Technology

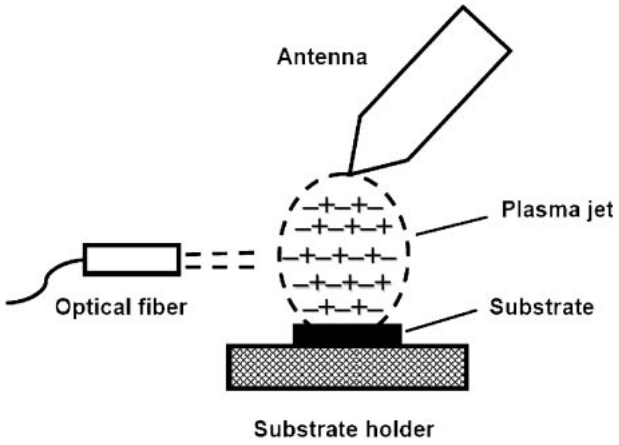

Fig. 1 Schematic representation of OES experimental set-up.

for the (111), (220) (311) and (400) reflections, respectively.

When OES is employed to measure the chemically reacted vapor species in the growth of diamond film, the optical source emitted by the plasma beam will penetrate the quartz window and lance, and will be transmitted by light to reach CCD array spectroscopy (B&WTek BTC112E). OES will acquire the resolution of 0.28 nm and the optical spectrum will range from 200 to 700 nm. Moreover, the computer software BWSpect, will be implemented to control the aforementioned OES system as shown in Fig. 1.

3. Results and Discussion

In this study, microwave plasma beam is employed to form stable, highly concentrated and ionized plasma. At the same time, the quantity of activated gas molecules and activated chemical radicals in the plasma will increase. The highly ionized plasma will cause self-biasing of potential drop on the substrate surface,[14] thus yielding diamond film of high nucleation density. However, the parameters of the plasma-activated gas used in diamond synthesis, such as type, concentration, electron state (molecule, radical, excited state and ionization state) and gassed species can be employed to derive directly the response mechanism of the nucleation process (nucleation density, orientation, structural defect and impurity density control).[15]

3.1 Optical emission spectroscopy

The result confirms that various CH_4 concentrations (0.2%–99%) can be used for synthesizing diamond film through MPJCVD. In the synthesis process, the emission spectrum can be extracted as shown in Fig. 2. As can be seen, the main optical emission spectra (400–700 nm) such as H, CH and C_2 will be generated in the diamond synthesizing process as illustrated in Table 1.[16] The relationships between CH and C_2 emission strength and CH_4 concentration are also discussed. The ratio of emission strength of CH and C_2 to optical emission strength of H_β can be employed to measure the concentration of the species excited by both CH and C_2. For different excited species, there exist close associations between emission strength ratio, species activation rate and concentration. For a species in an optically excited environment, the light emission strength ratio can accurately reflect

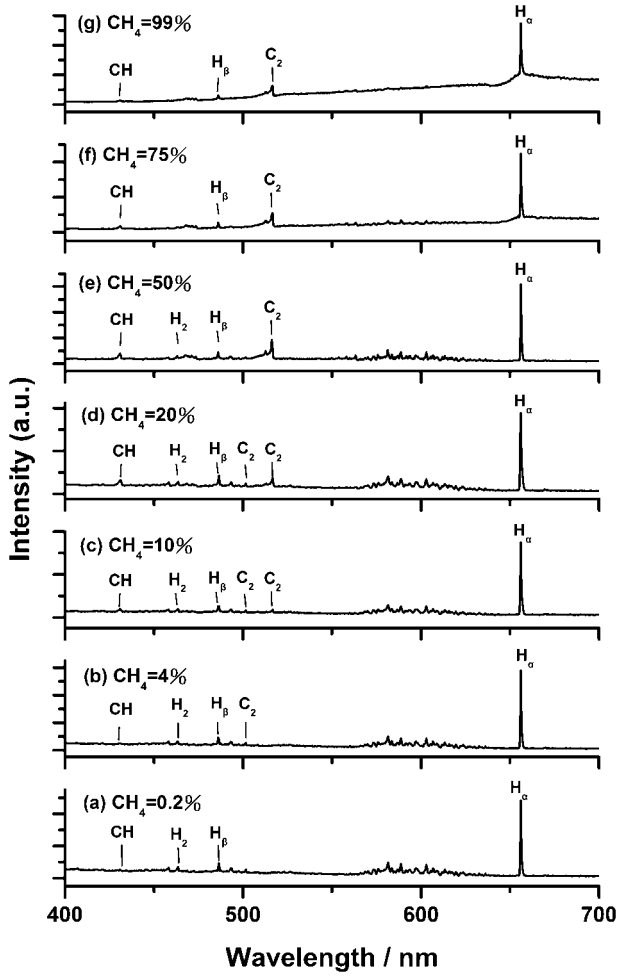

Fig. 2 Optical emission spectra of diamond growth at various CH_4 concentration.

Table 1 Optical emission lines observed in this work for a mixture of $CH_4 + H_2$.

Species	Electronic transition	Elecctoinc levels, E/eV	Wavelength, λ/nm
H_α	Balmer ($n = 3 \rightarrow 2$)		656.2
H_β	Balmer ($n = 4 \rightarrow 2$)		486.1
H_2	$G^1\Sigma_{g^+} \rightarrow B^1\Sigma_{u^+}$		462.9
C_2	Swan ($A^3\Pi_g \rightarrow X'^3\Pi_\mu$)		501.5
C_2	Swan ($D^3\Pi_g \rightarrow A^3\Pi_\mu$)	$2.59 \rightarrow 0.089$	516.1
CH	$A^2\Delta \rightarrow X^2\Pi$		431.4

the relationships between different concentrations of species.

Figure 3 illustrates the relationships between the light emission strength ratio of CH/H_β and C_2/H_β and main lattice plane of diamond film synthesized under different CH_4 concentrations. As can be seen, increase in CH_4 concentration will also enhance the emission strength of C_2/H_β. In addition, C_2/H_β is more sensitive than CH/H_β in terms of strength ratio. It is also found in this study that CH_4 concentration will increase with the growing light emission strength of C_2 in that CH_4 can substantially enhance plasma ionization and disassociation. Figure 3 shows the relationships between intensity ratios (111) and (220) and various concentrations after the lattice orientation of diamond film is detected by X-ray diffraction and standardized. As seen

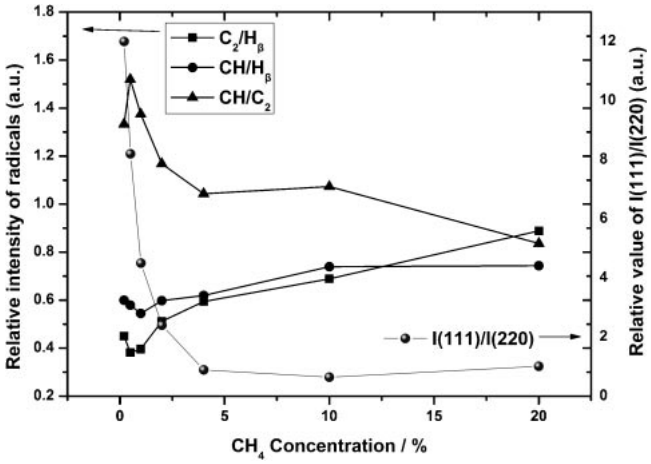

Fig. 3 Relationship between intensity ratios of I(111)/I(220), C_2/H_β, CH/H_β and CH/C_2 versus methane concentration.

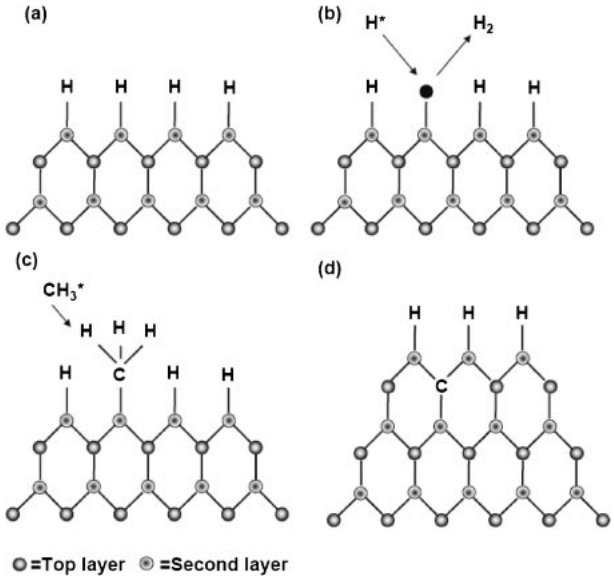

Fig. 4 Schematic presentation of surface processed during diamond growth.

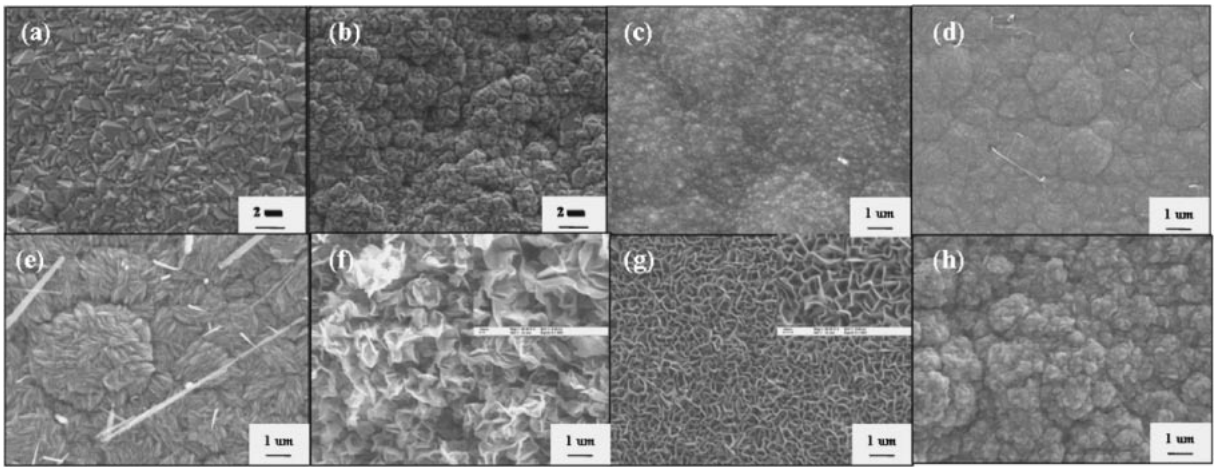

Fig. 5 SEM image of diamond growth at various CH_4 concentrations (a) 0.2%, (b) 1%, (c) 4%, (d) 10%, (e) 20%, (f) 50%, (g) 75% and (h) 99%.

in Fig. 3, the ratio between I(111)/I(220) decreases with increasing CH_4 concentration, and the rule governing the variation in strength ratio of CH/C_2 approximates the rule governing the variation in main lattice plane with concentration. D'Evelyn[17] discovered that C_2H_x contributes to the formation of (111) dominant crystalline surface in the growth of diamond film while CH_y contributes to the formation of surface other than (111). The carbon emission spectra of C_2 and CH can be employed to represent C_2H_x and CH_y respectively, and therefore the increase in CH/C_2 ratio may enhance the probability of lattice plane (111).

Experimental results reveal that excellent (111) dominant crystalline surface diamond film can be obtained in the plasma where optical emission intensity of radical is $H_\beta > CH > C_2$, and that CH is high while C_2 is low. With gaseous H in plasma excited, H^* activated species will be formed and be responsible for such tasks as etching non-diamond carbon and maintaining sp^3 structure of diamond surface. H^* species attacks C–H bond on the diamond surface to generate H_2 and detach itself from the diamond surface (Fig. 4(b)). At the same time, it will result in dangling bond appearing on the diamond surface. When the diamond surface is fully filled with CH_3^*, the precursor for diamond growth will be formed (Fig. 4(c)), and diamond film will grow (Fig. 4(d)).[18] Therefore, the desired main lattice plane of diamond film can be obtained by controlling the plasma parameters.

3.2 Growth and morphology of diamond films

Figure 5 shows the surface morphologies of diamond films grown at various CH_4 concentrations. The H/C ratio in the growth environment will increase with increasing CH_4 concentration while the facets geometry change from (111) to (220) (Fig. 3), and the grain size will be reduced to generate the twin crystal on the boundary. The surface morphology of the diamond will change from faceted into twinned (Fig. 5(b) and Fig. 6(b)). When CH_4 concentration rises by 4%, grain growth will be interfered by problems such

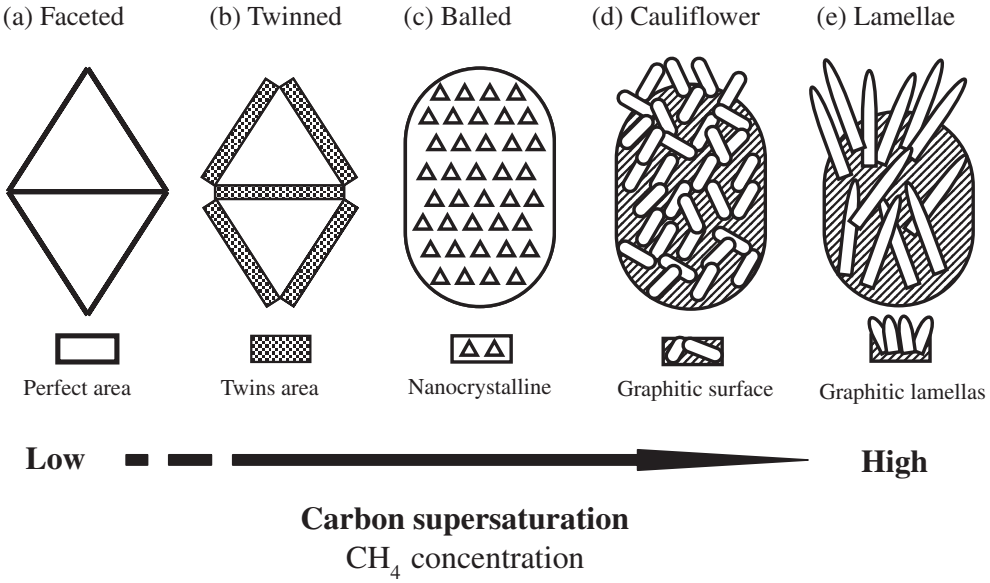

Fig. 6 Schematic drawing of microstructure of various CH_4 concentrations.

as supersaturation of hydrocarbons, less hydrogen atoms or by a decreasing surface mobility of the growth species. The rapid growth makes it more difficult to form the complete faceted surface, thus leading to the disappearance of diamond lattice plane, and the formation of balled surface, as shown in Fig. 5(c) (schema drawing on the Fig. 6(c)). When CH_4 concentration exceeds that of the environment by 10%, the surface morphology of diamond surface will be obviously subject to C_2/H ratio, thus transforming the morphology from a balled surface to that of cauliflower (Fig. 5(e)). Next, the film surface will undergo a series of changes from the thin lamella (<10 nm) graphite structure (Fig. 5(f)) to the regular lamella (<20 nm) graphite structure (Fig. 5(g)) and finally the balled graphite structure (Fig. 5(h)), as indicated in Fig. 6. It can be inferred from the above results that when CH_4 concentration is less than 10%, different surface morphologies of the diamond will be formed. During diamond growth, large quantities of hydrogen protons will effectively etch sp^2 carbon and stabilize sp^3 carbon, but decelerate diamond nucleation. With increase in CH_4 concentration, grain size will become smaller and nucleation will be accelerated. Once nucleation rate exceeds $10^7/cm^2$-s, nanocrystalline diamond film will appear.

C_2 species contributes to the formation of diamond phase and increases nucleation to develop nanocrystalline diamond film. On the other hand, H proton is capable of etching, activating and stabilizing diamond phase. Figure 7 shows the relationships between C_2/H_β ratio in optical emission intensity and surface morphologies of diamond films grown at varying CH_4 concentrations. From these figure it is evident that CH_4 concentration increases as C_2/H_β ratio of intensity increase (and CH/C_2 ratio of intensity decrease). According to the C_2/H_β ratio of intensity and SEM surface morphology image shown in Fig. 5, microcrystalline diamond (MCD) film is likely to grow in the plasma environment with C_2/H_β ratio of intensity below 0.51; nanocrystalline diamond (NCD) film is likely to grow when C_2/H_β ratio of intensity ranges from 0.51 to 0.69; cauliflower diamond film is likely

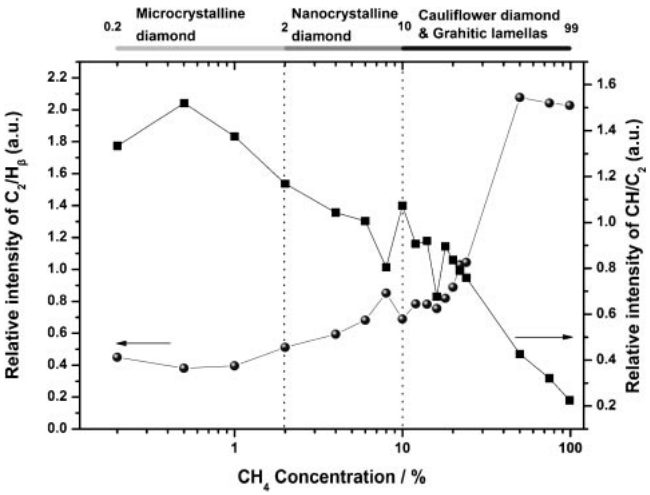

Fig. 7 Variation in nucleation rate and grain size versus CH_4 concentration during diamond growth.

to grow when C_2/H_β ratio of intensity ranges from 0.69 to 1.04; and lamella graphite diamond will be formed and later replaced by balled graphite when C_2/H_β ratio of intensity exceeds 2.

3.3 Analysis of the diamond films Raman spectra

Figure 8 shows Raman spectra of diamond films grown at various CH_4 concentrations. These diamond films include typical microcrystalline diamond film ($CH_4 = 0.2\%–2\%$), nanocrystalline diamond film ($CH_4 = 2\%–10\%$), cauliflower diamond film ($CH_4 = 10\%–20\%$), and lamella and balled graphite ($CH_4 > 50\%$). According to the Raman spectra, there are five characterization peaks at 1150, 1332, 1350, 1490 and 1580 cm^{-1}. In Fig. 8(a), the peak 1332 cm^{-1} is referred to as D_f-peak, which represents the characterization peak of sp^3 diamond. In Fig. 8(b), 1350 and 1580 cm^{-1} are called D-peak and G-peak, respectively, which represent the condition that sp^2 carbon structure and graphite structure are generate the crystal surface of the diamond film. In other

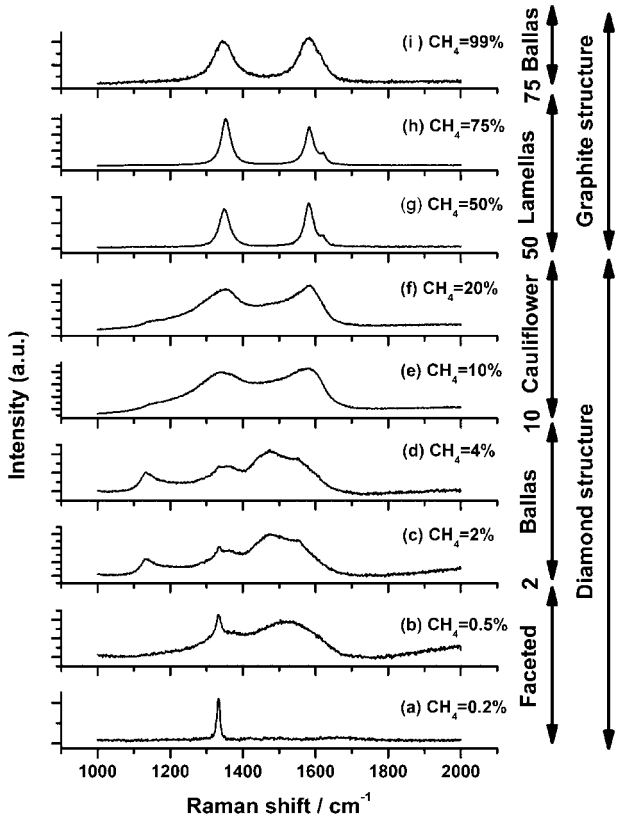

Fig. 8 Raman spectra of diamond films prepared at various CH_4 concentrations.

words, diamond quality will drop with increase in CH_4 concentration. Figure 8(c) show on 1332 cm^{-1} because the grain of nanocrystalline diamond film is so tiny that it cannot be measured by Raman spectroscopy within the range of 514 nm. Two characterization peaks of 1150 and 1490 cm^{-1} usually represent crystal phase of nanocrystalline diamond or sp^3 diamond structure.[19] The bonding form of characterization peaks D* and G* has not been clearly defined until Ferrari proved that characterization peaks 1150 and 1490 cm^{-1} represent respectively the transpolyacetylene (t-PA) formed by C=C bond stretching vibration (ν_1) and C–C bond stretching vibration (ν_2), which is bonded to carbon species on crystal surface and diamond film surface.[20] Therefore, these two characterization peaks are identified as signals generated by the transpolyacetylene contained in the nanocrystalline diamond film at the grain boundary. In Fig. 8(e)–(f), regarding the case where CH_4 concentration is less than 20%, the intensity of the Raman characterization peaks at 1350 and 1490 cm^{-1} will increase with rising CH_4 concentration. The result indicates that more disorderly carbon and transpolyacetylene will be produced as CH_4 concentration increases during the synthesis of diamond film. When CH_4 concentration exceeds 50%, the characterization peaks of typical D-peak and G-peak will appear (Fig. 8(g)–(i)).

4. Conclusions

Using plasma OES, this study diagnoses and measures the different conditions where diamond films are grown, and attempts to establish the plasma model for growing diamond film. Results show that species such as CH, C_2 and H_β contained in microwave plasma beam have significant influence on grain size, surface morphology and H/C carbon concentration. Optical emission spectra C_2 and CH can be employed to identify the presence of hydrocarbon species such as C_2H_x and CH_y. Therefore, increase in CH/C_2 ratio is likely to produce lattice plane (111). With decrease CH_4 concentration and H/C ratio in the growth environment, the diamond surface morphology will change from faceted into twinned, and finally into balled form when the diamond grain disappears at 2% CH_4 concentration. When CH_4 concentration exceeds that of the environment by 10%, the surface morphology will mainly be influenced by C_2/H ratio. The surface morphology will change from balled into cauliflower. When CH_4 concentration exceeds 50%, the film surface will undergo a series of changes from thin lamella graphite, regular lamella graphite to balled graphite in the end. The structural variation can also be measured by Raman spectroscopy. The Raman spectra prove the relevance of CH/C_2 concentration to surface morphology of diamond film.

Acknowledgements

Funding for this investigation was provided by the National Science Council, ROC under grant number NSC 96-2221-E-027-048.

REFERENCES

1) H. S. Liu and D. S. Dandy: *Diamond Chemical Vapor Deposition: Nucleation and Early Growth Stages*, (Noyes, Park Ridge, USA, 1995) pp. 14–17.
2) S. D. Wolter, B. R. Stoner, J. T. Glass, P. J. Ellis, D. S. Buhaenko, C. E. Jenkins and P. Southworth: Appl. Phys. Lett. **62** (1993) 1215–1217.
3) J. C. Angus and C. C. Hayman: Science **241** (1988) 913–921.
4) R. R. Burke and C. Pomot: Appl. Sur. Sci. **36** (1989) 267–277.
5) Y. Mitsuda, T. Yoshida and K. Akashi: Rev. Sci. Instrum. **60** (1989) 249–252.
6) D. G. Goodwin: J. Appl. Phys. **74** (1993) 6888–6894.
7) P. Redfern, D. A. Horner, L. A. Curtiss and D. M. Gruen: J. Phys. Chem. **100** (1996) 11654–11663.
8) K. Wu, E. G. Wang, Z. X. Cao, Z. L. Wang and X. Jiang: J. Appl. Phys. **88** (2000) 2967–2974.
9) T. G. McCauley, D. M. Gruen and A. R. Krauss: Appl. Phys. Lett. **73** (1998) 1646–1648.
10) D. Zhou, A. R. Krauss, T. D. Corrigan, T. G. McCauley, R. P. H. Chang and D. M. Gruen: J. Electrochem. Soc. **144** (1997) L224–L228.
11) A. Heiman, I. Gouzman, S. H. Christiansen, H. P. Strunk, G. Comtet, L. Hellner, G. Dujardin, R. Edrei and A. Hoffman: J. Appl. Phys. **89** (2001) 2622–2630.
12) M. Hiramatsu, K. Kato, C. H. Lau, J. S. Foord and M. Hori: Diam. Relat. Mater. **12** (2003) 365–368.
13) R. Haubner and B. Lux: Int. J. Refract. Met. Hard Mater. **20** (2002) 93–100.
14) S. Yugo, N. Ishigaki, K. Hirahara, J. Sano, T. Sone and T. Kimura: Diam. Relat. Mater. **8** (1990) 1406–1409.
15) Q. Yang, S. Yang, Y. S. Li, X. Lu and A. Hirose: Diam. Relat. Mater. **16** (2007) 730–734.
16) M. M. Larijani, F. L. Normand and O. Crégut: Appl. Sur. Sci. **253** (2007) 4051–4059.
17) M. P. D'Evelyn, J. D. Graham and L. R. Martin: Diam. Relat. Mater. **10** (2001) 1627–1632.
18) H. Kuzmany, R. Pfeiffer, N. Salk and B. Gunther: Carbon **42** (2004) 911–917.
19) T. R. Anthony: Vacuum **41** (1990) 1356–1359.
20) A. C. Ferrari and J. Robertson: Phys. Rev. B **63** (2001) 121405.